

# Thermo Physical Principles of Cogeneration Technology with Concentration of Solar Radiation

Peter Nesterenkov<sup>1(⋈)</sup> and Valeriy Kharchenko<sup>2(⋈)</sup>

 Al-Farabi Kazakh National University, Almaty, Kazakhstan stolkner@gmail.com
 Federal Scientific Agroengineering Center VIM, Moscow, Russian Federation kharval@mail.ru

**Abstract.** This paper considers the thermo physical principles of cogeneration technology with the use of silicon photocells working with a low concentration of solar radiation. The efficiency of the technology is enhanced by the use of photocells at a relatively high temperature and cooling with liquid, which makes it possible to obtain high-potential heat and transmit it to the heat carrier in counter flow mode of the coolant. Transportation of heat energy to a stationary storage system is realized under the influence of the pressure head formed by the temperature gradient along the height of the circulation circuit. A mathematical model is proposed for calculating the thermal energy of linear photovoltaic modules, taking into account the experimentally determined electric efficiency of commercially available silicon photocells.

**Keywords:** Photocells  $\cdot$  Optical concentrator  $\cdot$  Heat exchanger Energy storage system

# 1 Introduction

The widely available solar uncooled photovoltaic modules with silicon photocells (PV modules) which have an electrical efficiency of  $\approx 15\%$  emit more than 70% of the incoming solar energy into the environment in the form of heat. In coolant-cooled systems (photovoltaic-thermal modules, PVT), degree of conversion of solar energy is increased due to the utilization of thermal energy [1]. However, in such systems thermal energy is low potential, due to the negative effect of high temperature on the electrical efficiency of silicon photocells. The temperature of the coolant can be increased by using high-temperature two-junction GaAs or three-junction InGaP/InGaAs/Ge photocells [2]. At the same time, there are very few chemical elements Ga, As and In in the earth's crust, and the technology of manufacturing multitransitional photocells is complex and expensive.

The enormous technological potential of silicon photocells is far from exhausted. In work [3] Rosell and others at a 6-fold concentration from the cooled photocells obtained a total efficiency of  $\approx$ 60% and a temperature of the coolant at the outlet of about 61 °C. Engineers of the Cogenra Solar (Sun Power Corporation) at 8-fold

<sup>©</sup> Springer Nature Switzerland AG 2019
P. Vasant et al. (Eds.): ICO 2018, AISC 866, pp. 117–128, 2019. https://doi.org/10.1007/978-3-030-00979-3\_12

concentration of the sun received electricity productivity of  $\approx 100 \text{ W/m}^2$  and heat  $\approx 490 \text{ W/m}^2$  and for the first time proved the five-year payback of capital investments in the production of solar installations [4]. However, the high cost of installed capacity  $\approx \$1400/\text{m}^2$  restrains their commercialization. The task of delivering high-potential thermal energy to the storage system without significant energy costs and heat losses remains topical. In this work, we consider the scientific and technical principles of cogeneration technology with the use of silicon photocells with a low concentration of solar radiation and the transportation of the resulting hot coolant to the storage system with minimal energy costs.

## 2 Methods and Calculations

The concept of the technology is based on the generation of electricity and heat by silicon photocells relatively large area with increased density of solar radiation and an elevated temperature on the surface, followed by the transport of high-grade heat released to the integrated energy storage system. The continuous generation of electric power is being realized in the technological combination of wind generation and solar generation in the space of a common carrying platform. This is facilitated by the natural phenomenon of increasing wind speed with the absense (cloudy periods, nighttime etc.) of the sun. The concept is implemented in budget solar-wind systems with concentration of solar radiation (CSWs). In all standard designs, they include a supporting structure, carrying platform, an optical concentrator, PV modules, circulation circuits with cooled photocells, a circulation circuit with a heat exchanger and a heat accumulator, wind generators, integrated energy storage system, power management and power delivery unit. The most capital-intensive are the supporting structure, carrying platform with an optical concentrator and the storage system for electrical and thermal energy.

## 2.1 Design of the Load-Bearing Platform

Lightweight load-bearing platform is made of a standard metal profile with the use of engineering technologies for the construction of solid truss structures. Dynamic stability of the bearing platform in conditions of turbulent wind currents is provided by using four points of support and two pass-through bearings for heat carriers. Due to the orientation of the longitudinal axis at an angle to the horizon and the counter position of the walls of the pv modules along them, a protective thermal layer is formed from the convection of the hot surfaces placed below [5]. Figure 1 presents a version of the CSWs with one section of the carrier platform, and a system for measuring technological parameters. Step-by-step tracking of the carrier platform behind the sun and seasonal adjustment for the height of the sun are carried out using trackers according to the controller program.

The total peak power of the CSWs (two sections) is  $\approx 11$  kW and total capacity is calculated from the condition of full provision of the average farmhouse with electricity and heat in the summer. During winter heating, solid fuel boilers can be connected to the energy storage system through integrated interface. The equipment is delivered to





Fig. 1 CSWs with one section concentrator and measuring system

the installation site in twenty-foot containers, which serve as a supporting structure and a hermetically sealed box for the energy storage system and monitoring devices.

## 2.2 Optical Concentrators

For mirrors, relatively thin glass with a low iron content is used, which reduces the unit cost of optical concentrators to  $\approx\!\!15/m^2.$  In further, it is planned to switch to Alanod Silver mirror films (Germany) with a reflection coefficient of  $K_r\approx 0.95$  on a thin metal substrate made of aluminum or copper [6]. Design of concentrators are developed in accordance with the laws of geometric optics using computer modeling in Autodesk Inventor software. Figure 2 shows an optimal distribution of reflected solar rays in the working area of photocell surfaces.



Fig. 2 Optical scheme of solar-wind systems with concentration of solar radiation

When the sun moves across the sky with angular velocity  $\omega \approx 2\pi/24 \cdot 0$  rad/min during the shutdown time of the tracker engine  $\tau$ , the solar beam is displaced in space from A to  $A_1$ . If the distance between pv modules and mirrors is denoted by R, we obtain the displacement of the reflected light spot along the wall surface  $\Delta = \tau \cdot R \cdot (2\pi/24 \cdot 60)$ , which is shown in Fig. 3.

At a distance  $R \approx 1.5$  m, displacement for one minute is equal to  $\Delta \approx 6$  mm. To account for the effect of displacement, the transverse size of the light spot is chosen to be larger than the size of the photocells b mm, from which the minimum transverse mirror size min  $b_Z \geq (b + \Delta)$  is determined. The optimal reflecting surface is a

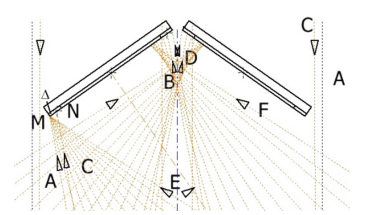


Fig. 3 Reflected solar rays on photocell surfaces

parabolic surface with a focal length f, whose analytical expression in the XY coordinate system has the form:  $(X + X_1)^2 = 4 \cdot f \cdot Y$ . The first mirror of the concentrators is at a distance  $X_1$  from the coordinate axis (Table 1).

Tube 1 Coolemaces of minors												
№	1	2	3	4	5	6	7	8	9	10	11	12
X, m	0.285	0.418	0.502	0.702	0.842	0.982	1.122	1.262	1.402	1.542	1.682	1.822
V m	0.017	0.029	0.053	0.082	0.118	0.161	0.210	0.265	0.328	0.396	0.472	0.553

Table 1 Coordinates of mirrors

Modeling allowed to determine the optimal value of the geometric coefficient - the ratio of the area of the aperture of the concentrator to the area of the mirrors  $K_g\approx 0.96$ . The transmission of solar radiation by the optical system depends on the total thickness of the mirrors and the protective thermal glasses. For example, with a total thickness of  $\approx \! 10$  mm, up to  $\approx \! 8\%$  of solar energy is absorbed [7]. Therefore, the proposed optical concentrator uses glass with a thickness of no more than 2 mm. This, in turn, limits the size of the optical elements due to the mechanical strength. As a result, the total transmission coefficient of solar radiation was increased to  $K_d\approx 0.95$ . Thin, relatively expensive thermal glasses have self-protection against hail and other large atmospheric precipitations. Innovative technical solutions allowed to increase optical efficiency up to  $C_o=K_g \cdot K_r \cdot K_d\approx 0.83$ . Taking into account the inevitable contamination of the optics, its real value is reduced to  $\approx \! 0.8$ . Accordingly, the optical concentration for twelve mirrors is  $C_{ok}\approx C_o \cdot N = 0.8 \cdot 12 \approx 9.7$ .

Due to the orientation of the pv modules at an angle to the horizon and counterangled  $\varphi 0$  to each other, as shown in Fig. 3, the hot air flow is directed up along the adjacent walls and forms a thermal protective layer, which reduces the heat loss by  $\approx 12\%$  compared to conventional convection [8].

In accordance with the Stefan-Boltzmann law, the surfaces of pv modules emit heat flux into space [9]:

$$dQ = \epsilon \sigma_0 \Big[ (T/100)^4 - (T_0/100)^4 \Big] F \int_0^{\pi} d\phi$$
 (1)

where -  $\epsilon$  and T - reduced blackness and temperature of the surface of the radiating body;  $\sigma_0 = 5,67 \cdot 10^{-8} W/(m^2 \cdot K^4)$  - Stefan-Boltzmann constant;  $T_0$  - ambient temperature; F - surface area;  $\phi$  - solar radiation angle.

In the case of screening of the walls of adjacent pv modules, the integration of expression (1) is carried out in the interval of angles  $(\pi - \phi_0/2; \pi)$ . Other things being equal, the value of the radiation loss ratio of mutually screened and freely placed surfaces is: :  $\approx \epsilon \sigma_0 (T/100)^4 (\pi/3)/\epsilon \sigma_0 (T/100)^4 \pi \approx 0.33$ . The back-to-back inclusion of the walls with photocells working with radiation concentration leads to a reduction of thermal losses by radiation by 33%.

One of the problems of operating optical concentrators during autumn-winter period is the need for cleaning after snowfalls. In the proposed variant, unlike analogues, the working surfaces of pv modules are closed from atmospheric precipitation, and the thermal radiation from the surface of the thermal battery, pv modules and heat exchanger keeps the mirror temperature above zero. As a result, the snow does not linger and rolls down, as shown in Fig. 4.



Fig. 4 Operating during snowfall

## 2.3 Linear PV Modules

In the innovative method of increasing the efficiency of heat transfer, the physical effect of increasing the heat transfer coefficient with increasing medium temperature and discharging heat received from solar cells in the countercurrent mode to the second heat carrier is used.

However, it is necessary to solve the problem of ensuring reliable operation of photocells at elevated temperature and alternating thermal loads in conducting contact areas. Therefore, market photocells with a relatively low degree of degradation are selected under the specified conditions. These criteria are met by relatively cheap high-quality Maxeon solar cells from SunPower Corporation [10]. Under standard conditions, they have a peak power of  $\approx\!3.4$  W and temperature power factors  $k_P\approx 0.011\,\text{W}/^0\text{C}$  and voltages  $k_U\approx 0.0018\,\text{V}/^0\text{C}$ . At the maximum power point, voltage and current are  $U_m\approx 0.57\,\text{V}$  and Im  $\approx 5.8$  A. Under operating conditions with a low concentration (up to ten times) at a standard temperature of  $\approx\!25\,^{\circ}\text{C}$ , a peak power of  $\approx\!19$  W has been obtained [11].

Silicon photocells with low light intensity within the theoretical Shockley model are described by an equivalent circuit of a diode with a photocurrent generator  $I_{Ph}$  and an

internal series resistance  $R_S$  [12]. The intensive cogeneration mode changes the representation of photocells as energy converters and requires the modernization of the equivalent diode circuit, adding to it the heat generator Q and the radiation source, as shown in Fig. 5. Switches S<sub>1</sub> and S<sub>2</sub> are necessary for the transfer of photocells to shortcircuit with I<sub>SC</sub> current, idle mode with V<sub>OC</sub> voltage, or mode with external load R<sub>P</sub>.

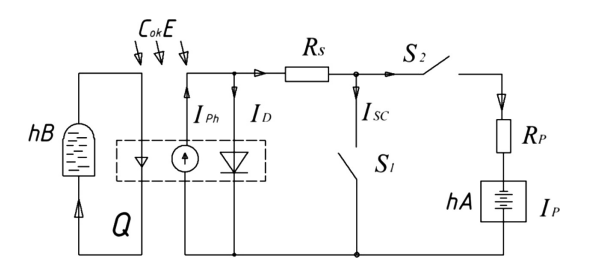


Fig. 5 Equivalent electrical circuit of CSWs

Under the influence of the radiation  $C_{ok} \cdot E$ , the photocell generates a photocurrent I<sub>Ph</sub> directed to the chemical accumulators hA, and the heat flux transported to the thermal energy storage system hB. Balance of power released by photocells is:

$$C_{ok} \cdot E \cdot S = G \cdot Cp \cdot (t_{out} - t_{in}) + P + W$$
 (2)

where S - area of photocells, m<sup>2</sup>; G - coolant flow, kg/s; C<sub>p</sub> - specific heat of the liquid,  $J/(kg \cdot K)$ ;  $t_{out}$  and  $t_{in}$  - output and inlet temperature of the coolant liquid, K; P - electric power, allocated by photocells, W; W - heat losses, W.

The operation of photocells with cogeneration is described by the electric energy  $\eta_e$ and the thermal efficiency  $\eta_T$ :

$$\eta = \eta_e + \eta_T = [I \cdot V + Q_T]/(C_{ok} \cdot S \cdot E)$$
 (3)

I and V - current and voltage at the maximum power point; Q<sub>T</sub> - useful thermal power, W; C<sub>ok</sub> - optical concentration; E - intensity of direct solar radiation, W/m<sup>2</sup>; S - area of photocells, m<sup>2</sup>.

Engineering method for calculating the efficiency of pv modules is based on experimental studies of thermal losses by cooled walls. During the transfer of solar energy to the heat carrier, the internal structure of the photocells and the shape of the heating source are not taken into account. This conclusion is the basis for the method of physical modeling of heat exchange processes. Instead of the sun and a complex tracking system, a thin electric-heated foil of nichrome is used. Between the foil and the wall is a heat-conducting adhesive, as for photocells. Thus, a convenient tool has been obtained for studying the influence of various design factors and external conditions on the thermal efficiency of pv modules. Figure 6 shows a mobile stand, which allows to standardize the testing process of the developed linear pm modules and carry out the adjustment of technical characteristics.





Fig. 6 Test bench for determining heat losses in flat channels of pv modules

The results of physical modeling studies over a wide range of changes in the external conditions of heat exchange between the channel and the coolant show that at an average coolant temperature of  $\leq 45$  °C, the thermal losses do not exceed  $\approx\!37\%$  [13]. It follows from this that the share of useful thermal power transmitted through the walls to the heat carrier is not less than  $\approx\!63\%$ . We take it as a boundary in the mathematical model for calculating the thermal power. With the known efficiency of the photocells and the radiation value  $\approx\!\!N\cdot C_{ok}\cdot E$ , and  $\varkappa\approx (E+E_d)$ , we obtain an analytical expression for determining the useful thermal power carried away by the coolant of a two-sided pv module

$$q_1 + q_2 = 0,63 \cdot E \cdot [N \cdot C_{ok} \cdot (1 - \eta_1) + (1 + E_d/E)(1 - \eta_2)]$$
 (4)

The temperature of the photocells is determined from the solution of the classical thermo physical problem - temperature distribution by the wall thicknesses with boundary conditions of the second kind on the outer walls  $q_1$  = const and  $q_2$  = const; and boundary conditions of the third kind on the inner walls  $q_1$  =  $\alpha_1$  ( $t_{c1}$  – t) and  $q_2$  =  $\alpha_2$  ( $t_{c2}$  – t) [14]. The heat transfer coefficients at the inner walls  $\alpha_1$  and  $\alpha_2$  are the average along the length of the channel. Figure 7 shows the calculation scheme.

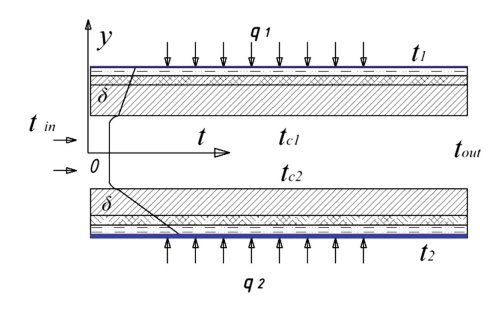


Fig. 7 The scheme of calculating photocells temperature

The thickness of the photocells and intermediate layers  $\delta_i$  is not given to scale. The axis of the coordinate passes along the axis of the channel. The process of heat exchange is stationary. The specific heat of the liquid  $C_p$  is taken at the average temperature of the liquid in the channel.

The heat flow passes successively through a thermoplastic sealant of thickness  $\delta_1$ , an oxidized layer  $\delta_2$ , a wall  $\delta_3$  and a boundary layer along the walls  $\delta_4$ . At the channels input goes coolant liquid with a mass flow rate G and a temperature  $t_{\rm in}$ . Taking into account the accepted assumptions, we obtain the following equations, from which the local temperature of photocells on the walls is determined:

$$\begin{split} T_1 &= t \ + q_1 \bigg( \frac{1}{\alpha_1} + \sum \frac{\delta}{\lambda} \bigg) \\ T_2 &= t \ + q_2 \bigg( \frac{1}{\alpha_2} + \sum \frac{\delta}{\lambda} \bigg) \end{split} \tag{5}$$

where  $t_1$  and  $t_2$  - temperatures of the outer walls (photocells); t - temperature of the coolant (liquid);  $\delta/\lambda$  - thickness and thermal conductivity of the sealant, oxidized layer and metal wall;  $\alpha_1$  and  $\alpha_2$  are the heat transfer coefficients on the inner surface of the walls.

The temperature of the liquid in the channel of length L and width f varies along the flow. The amount of heat discharged by the walls into the liquid in any section of the channel f dx goes to an increase in the temperature of the liquid by an amount dt, from which we write the heat balance equation in the form:

$$q_1 + q_2 = [\alpha_1(t_{c1} - t) + \alpha_2(t_{c2} - t)]fdx = C_pGdt \tag{6}$$

Heat transfer coefficients  $\alpha_1$  and  $\alpha_2$  are averaged over the entire surface of the walls. Since the heat flux is constant, Eq. (6) with separable variables has an analytical solution:

$$t = t_{in} + \frac{q_1 + q_2}{C_n G} fX \tag{7}$$

From Eqs. (5) and (7) we obtain an expression for calculating the temperature of photocells at a distance X from the entrance to the channel:

$$\begin{split} t_1 &= t_{in} + \frac{q_1 + q_2}{C_p G} fX + q_1 \left( \frac{1}{\alpha_1} + \sum \frac{\delta}{\lambda} \right) \\ t_2 &= t_{in} + \frac{q_1 + q_2}{C_p G} fX + q_2 \left( \frac{1}{\alpha_2} + \sum \frac{\delta}{\lambda} \right) \end{split} \tag{8}$$

The potential possibility of withdrawing the heat power emitted by photocells by the liquid is determined from the inequality:

$$0,63 \cdot E \cdot [C_{ok} \cdot (1 - \eta_1) + (1 + E_d/E)(1 - \eta_2)] \le S \cdot \left[ \frac{(t_1 - t)}{R_1} + \frac{(t_1 - t_0)}{R_2} \right]$$
(9)

where  $R_1$  and  $R_2$  - thermal resistances to the heat flux directed from photocells with temperature  $t_1$  to the heat carrier with temperature t and into the environment with temperature  $t_0$ , respectively, equal to  $R_1 = \frac{\delta_1}{\lambda_1} + \frac{\delta_2}{\lambda_2} + \frac{\delta_3}{\lambda_3} + \frac{1}{\alpha_1}$  and  $R_2 = \frac{\delta_4}{\lambda_4} + \frac{\delta_c}{\lambda_c} + \frac{1}{\alpha_\beta}; \lambda_1, \lambda_2, \lambda_3$  and  $\lambda_c$  - thermal conductivity of the thermoplastic sealant, oxide film and aluminum, respectively;  $\delta_4$ ,  $\delta_c$  and  $\lambda_4$ ,  $\lambda_c$  - thickness and thermal conductivity of EVA film and heat-resistant glass;  $\alpha_B$  - average heat transfer coefficient of the ambient air along the channel length;

Let us estimate the order of magnitude in the expression for the thermal resistance to the heat flux. When the thermal conductivity of the thermoplastic sealer is  $\lambda_1 \approx 0$ , 12 W/m · K and 0.1 mm thick, its thermal resistance is  $\approx 0,0001/0,12 = 8 \cdot 10^{-4}$  m<sup>2</sup> · K/W. A layer of aluminum oxide with thermal conductivity  $\lambda_2 \approx 2$  W/m · K and a thickness of  $\approx 0.1$  mm has a thermal resistance  $\approx 0,5 \cdot 10^{-4}$  m<sup>2</sup> · K/W. The thermal resistance of the aluminum walls of the channel is  $0,002/195 = 0,02 \cdot 10^{-4}$  m<sup>2</sup> · K/W. The flow of heat carriers in flat channels at a flow rate  $G \approx 0.017$  kg/s is close to a laminar flow and the heat transfer coefficient is  $\approx 370$  W/m<sup>2</sup> · K. As a result, the total thermal resistance  $R_1 \approx (0,8+0,05+0,002+2,8) \cdot 10^{-3}$  m<sup>2</sup> · K/W.

Figure 8 shows the results of the calculation of the temperature of photocells operating with low concentration of the sun. The graphs indicate the possibility of

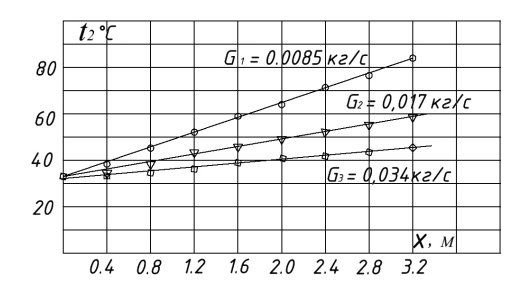


Fig. 8 Graphs of temperature variation of photocells along the channel wall as a function of liquid flow rate

flexible control of the temperature of the photocells by changing the flow rate of the liquid. In closed loop circuits, the temperature of the photocells is maintained at the required level due to the discharge of excess heat in countercurrent mode to the heat exchanger of the heat exchanger circuit.

The next step is to determine the total length of the channels of the pv modules. Denote  $\Delta t_j$  - difference between the temperature of the photocells on the channel walls and the standard operating temperature of 25 °C. At a temperature coefficient  $k_U$ , the voltage drop across the  $j_{th}$  photocell along the channel is determined from the expression:  $\Delta U_i \approx k_U \cdot \Delta t_i$ . The total value of the voltage loss of the series-connected

photocells is, respectively:  $U_T = \sum k_U \cdot \Delta t_j$ . Taking into account the value of the voltage at the point of maximum power  $U_m \approx 0.57$  and the need to maintain an optimum charge voltage of chemical accumulators  $U_a \approx 14.2$  V, the minimum number of photocells connected in series is determined:  $n \approx (U_a + U_T)/U_m$ . To compensate resulting losses of voltage, additional photocells are introduced - one in the primary channels (in the direction of the coolant motion)  $(n_1 = n + 1)$  and three into the secondary channels  $(n_2 = n + 3)$ . From this we get the value of the total length of the connected channels:  $L_F \approx (n_1 + n_2) \cdot 0.126$ .

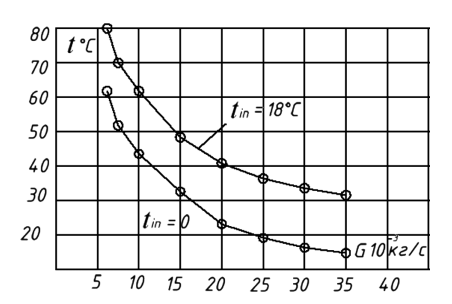


Fig. 9 Graph of the change in the outlet temperature of the liquid in the channel depending on consumption

A positive property of the serial connection of the channels along the heat carrier is the possibility of obtaining a hot liquid at the outlet. Figure 9 shows the liquid temperature at the outlet of the channel, depending on the flow rate and inlet temperature, obtained in accordance with the expression (8) at X = L.

In the proposed cogeneration systems, for the first time was put forward the idea of using the received heat energy (at solar energy systems) not only for its direct purpose, but also for performing mechanical work on the natural transportation of hot liquid from the heat exchanger to the energy storage system [14]. The realization of this idea is shown schematically in Fig. 10.

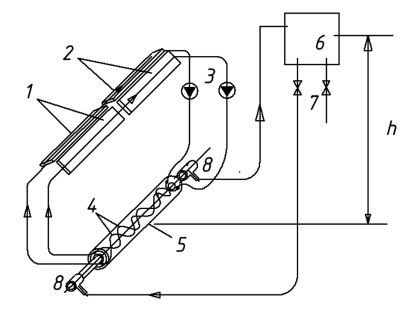


Fig. 10 Hydraulic circuit of the CSWs

The heat accumulator 6 is placed at a height h relative to the heat exchanger 5 and a temperature gradient is created between them, leading to a difference in the density of the liquid in the supply and descent pipelines of the closed circulation loop.

As a result, similar to the processes in the residential heating system, a dynamic pressure head appears that creates a natural flow of hot liquid to the heat accumulator:

$$\Delta P = gh \left( \rho_T - \rho_0 \right) \tag{10}$$

where  $\Delta P$  is the dynamic head, Pa; g - free fall acceleration, 9.81 m/s<sup>2</sup>; h - distance between the centers of the linear heat exchanger and the heat accumulator, m;  $\rho_o$  and  $\rho_r$  - density of hot and cold coolant, kg/m<sup>3</sup>.

With a temperature gradient of  $\approx 60$  °C, difference in density of the liquid is  $(\rho_T - \rho_o) \approx 14 \text{ kg/m}^3$ . At  $h \approx 4$  m dynamic pressure is  $\Delta P = g \cdot h \cdot (\rho_T - \rho_o) \approx 545$  Pa which is quite enough for carrying out the transportation of thermal energy from the movable pv modules to the stationary thermal accumulator through the through-channels of the support bearings. In the steady-state regime of natural fluid flow, the dynamic head  $\Delta P$  is equal to the sum of the hydraulic resistances in the channel of the heat exchanger  $\Delta P_T$  and the descending and lifting pipeline  $\Delta P_{TP}$ . Hot water during a sunny day accumulates in a heat-insulated thermal accumulator, the volume of which corresponds to the system capacity. The separation of the circulation circuits allowed to solve the problem of maintaining the necessary pressure in the flat channels of the pv modules and the circulation circuit with the charging of the consumable service water.

# 3 Conclusions

Using the example of designing low-power plants that are most in demand among farmers, the use of heat transfer laws in the processes of solar energy conversion using silicon cells of relatively large area can be traced. There is an optimal combination of the values of the concentration of solar radiation and the intensity of cooling of solar cells with liquid heat carriers, which allow the maximum amount of electrical and thermal energy to be generated per unit of aperture area of the installations, and a decrease of one value automatically leads to growth of another.

The property of the internal relationship between the electrical and thermal efficiency of photocells is particularly important in the creation of budget cogeneration plants for heating, use for energy supply of farms and desalination of water. For the first time reliable technology of transportation of high-potential heat released by photocells to the storage system under the influence of dynamic head, formed due to the temperature gradient in the heat exchanger circulation circuit, is realized. The results of physical simulation of heat exchange processes with the use of full-scale flat channels of pv modules made it possible to develop an engineering technique for calculating the productivity of linear pv modules for generation of thermal energy.

# References

- Chow, T.T.: A review on photovoltaic/thermal hybrid solar technology. Appl. Energy 2(87), 365–379 (2010)
- Kribus, A., Raftori, D., et al.: A miniature concentrating photovoltaic end thermal system. Energy Convers. Manag. (47), 3582–3590 (2006)
- 3. Al-Baali, A.A.: Improving the power of f solar panel by cooling and light concentrating. Solar Wind Technol. 4(13), 241–245 (1986)
- Forbes Marshall Ltd. http://www.forbesmarshall.com/solar\_cogeneration.aspx. Last accessed 21 Jan 2018
- Nesterenkov, A.G., Nesterenkov, P.A., Nesterenkova, L.A.: Innovative patent of the Republic of Kazakhstan №30003. A way of converting solar radiation into electrical and thermal energy and an installation for realizing the method (2015)
- 6. Alanod GmbH & Co. Homepage. http://www.alanod.com. Last accessed 21 April 2018
- Chea, L.C., Håkansson, H., Karlsson, B.: Performance evaluation of new two axes tracking pv-thermal concentrator. J. Civil Eng. Arch. 12(73), 1485–1493 (2013)
- Nesterenkov, P.A., Nesterenkov, A.G., Nesterenkova, L.A.: Fundamentals of designing hybrid concentrator solar systems. In: 12th International Conference on Concentrator Photovoltaics (CPV-12), Germany (2016)
- 9. Blokh, A.G., Zhuravlev, Yu.A., L.N. Ryzhkov. Handbook: Heat Exchange by Radiation, 1st edn. Energoatomizdat, Moscow (1991)
- 10. Sunpower Corporation. Homepage. http://www.sunpower.com last accessed 21 April 2018
- Nesterenkov, P.A., Nesterenkov, A.G.: Cogeneration Solar Systems With Concentrators of Solar Radiation. Handbook of Research on Renewable Energy and Electric Resources for Sustainable Rural Development. 1st edn. IGI-Global, Pennsylvania (2018)
- 12. Shockey, W., Queisser, H.: Solar concentrators. Appl. Phys. (1961)
- 13. Mikheev, M.A., Mikheeva, I.M.: Fundamentals of Heat Transfer. Handbook: Energy, 3rd edn. Energoatomizdat, Moscow (1977)
- 14. Nesterenkov, P.A., et al.: Cogeneration systems with radiation of solar concentration a new type of equipment for solar energy. Energy of the future: innovative scenarios and methods of their implementation. In: Abykayev, N.A., Zhumagulov, B.T. (eds.) Proceedings of Word Congress of Engineers and Scientists, Astana, vol. 3, pp. 266–273 (2017)